10-Gb/s Wavelength and Pulse Format Conversion Using Four-Wave Mixing in a GaAs Waveguide

Paveen Apiratikul, *Student Member, IEEE*, W. Astar, Gary M. Carter, *Fellow, IEEE*, and Thomas E. Murphy, *Senior Member, IEEE*

***Abstract*—We demonstrate the simultaneous conversion of wavelength and nonreturn-to-zero to return-to-zero (RZ) format at 10 Gb/s, using four-wave mixing in a passive GaAs bulk-waveguide. A conversion efficiency of −28 dB (idler output relative to signal output) and a conversion bandwidth of 48 nm could be achieved in this waveguide, which was fabricated in a single photolithographic step. The conversion efficiency is also characterized and compared with simulated results. The converted RZ on–off keying (RZ-OOK) signal demonstrated a 10^{-9} bit-error-rate receiver sensitivity penalty of 1 dB relative to baseline RZ-OOK.**

***Index Terms*—Integrated optics, nonlinear optics, optical frequency conversion, optical mixers.**

I. Introduction

NONLINEAR optical processing is being actively investigated for such functionalities as wavelength conversion, pulse-format conversion, demultiplexing, and optical sampling. Several nonlinear optical techniques have been proposed and demonstrated for wavelength and format conversion including four-wave mixing (FWM) or cross-phase modulation (XPM) in nonlinear fiber [1], semiconductor optical amplifiers (SOAs) [2], and silicon nanowires [3], [4].

GaAs–AlGaAs waveguides are a promising platform for performing wavelength and format conversion, with advantages including broadband transparency throughout the telecommunication band, the flexibility to engineer the bandgap and incorporate heterostructure multilayers, and the potential for integration with high-speed electronics. In the 1550-nm wavelength regime, the optical Kerr coefficient of GaAs is approximately 1000 times stronger than that of silica and 4 times larger than that of crystalline silicon [5]. This enables reasonable nonlinear efficiency in GaAs waveguides, even without using submicrometer mode sizes. Third-order nonlinear effects have been observed in several GaAs–AlGaAs devices including waveguides [6], directional couplers [7], microring resonators [8], photonic crystal cavities [9], and nanowires [10].

Manuscript received November 03, 2009; revised January 26, 2010; accepted March 20, 2010. Date of publication April 08, 2010; date of current version May 21, 2010.

P. Apiratikul and T. E. Murphy are with the Department of Electrical and Computer Engineering, University of Maryland, College Park, MD 20742 USA (e-mail: tem@umd.edu).

W. Astar is with the Laboratory for Physical Sciences (LPS), College Park, MD 20740 USA, and also with also with the Center for Advanced Studies in Photonic Research (CASPR), Baltimore, MD 21250 USA.

G. M. Carter is with LPS, CASPR, and the Department of Computer Science and Electrical Engineering, University of Maryland, Baltimore County (UMBC), Baltimore, MD 21250 USA.

Color versions of one or more of the figures in this letter are available online at http://ieeexplore.ieee.org.

Digital Object Identifier 10.1109/LPT.2010.2047009

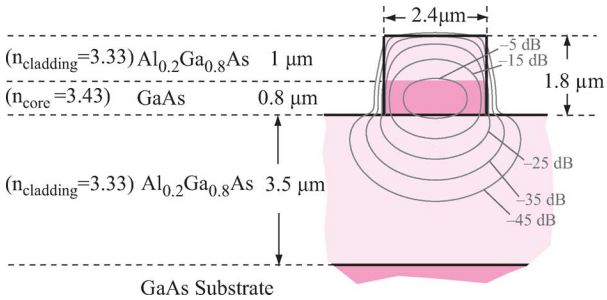

Fig. 1. Cross-section of the GaAs–AlGaAs bulk-waveguide, showing the layer compositions, refractive indices, and calculated optical mode.

Although nonlinear effects including self-phase modulation and FWM have been observed in GaAs–AlGaAs waveguides, to date there have been no clear demonstrations of communication applications, and no reports of data performance metrics such as eye diagrams or bit-error-rate (BER) receiver sensitivity. In this report, we investigate the efficacy of all-optical, simultaneous wavelength and nonreturn-to-zero to return-to-zero (NRZ-to-RZ) format conversions at 10 Gb/s, using FWM in a GaAs–AlGaAs bulk-waveguide. We achieved a conversion efficiency of −28 dB, and receiver 10^{-9} BER power penalty of 1 dB relative to baseline RZ.

II. Experiment

Fig. 1 depicts the GaAs ridge waveguide used in this experiment, which was patterned using photolithography and an inductively coupled plasma etching. The waveguide was cleaved to a length of 4.5 mm, and silicon–nitride antireflection coatings were deposited on both facets. The calculated mode contours are superposed on the cross-section in Fig. 1, yielding an effective area of 1.8 μm^2.

The nonlinear optical interaction between the pump, signal, and idler is described by the following propagation equations [11]:

$$\frac{dP_p}{dz} = -\alpha P_p - \frac{\beta_{2PA}}{A_{eff}}(P_p + 2P_s + 2P_i)P_p - 4\frac{\omega n_2}{cA_{eff}}P_p\sqrt{P_sP_i}\sin\theta - 2\frac{\beta_{2PA}}{A_{eff}}P_p\sqrt{P_sP_i}\cos\theta \quad (1a)$$

$$\frac{dP_s}{dz} = -\alpha P_s - \frac{\beta_{2PA}}{A_{eff}}(2P_p + P_s + 2P_i)P_s + 2\frac{\omega n_2}{cA_{eff}}P_p\sqrt{P_sP_i}\sin\theta - \frac{\beta_{2PA}}{A_{eff}}P_p\sqrt{P_sP_i}\cos\theta \quad (1b)$$

$$\frac{dP_i}{dz} = -\alpha P_i - \frac{\beta_{2PA}}{A_{eff}}(2P_p + 2P_s + P_i)P_i + 2\frac{\omega n_2}{cA_{eff}}P_p\sqrt{P_sP_i}\sin\theta - \frac{\beta_{2PA}}{A_{eff}}P_p\sqrt{P_sP_i}\cos\theta \quad (1c)$$

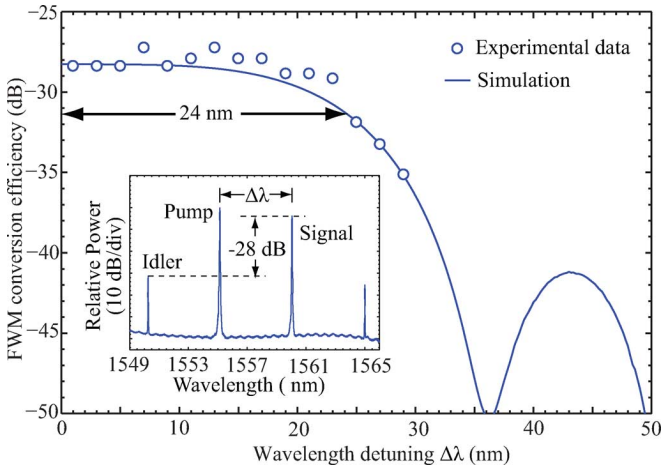

Fig. 2. Measured and simulated conversion efficiencies as wavelength detuning. The inset shows the output FWM spectrum after the GaAs waveguide with the wavelength detuning of 5 nm.

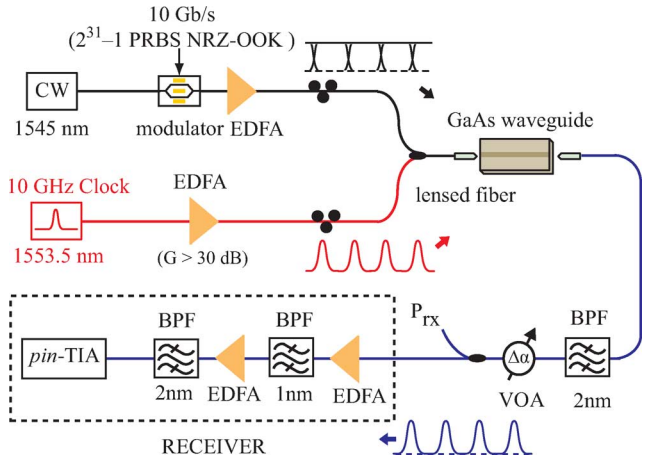

Fig. 3. Setup used for 10-Gb/s wavelength and format conversion. (P_{rx}: receiver power; VOA: variable optical attenuator; *pin*-TIA: p-i-n photodiode and transimpedance amplifier; PRBS: pseudorandom bit sequence.).

$$\frac{d\theta}{dz} = (k_s + k_i - 2k_p) + \frac{\omega n_2}{cA_{\text{eff}}}(2P_p - P_s - P_i) + \frac{\omega n_2}{cA_{\text{eff}}}\left(P_p\sqrt{\frac{P_s}{P_i}} + P_p\sqrt{\frac{P_i}{P_s}} - 4\sqrt{(P_sP_i)}\right)\cos\theta + \frac{\beta_{2\text{PA}}}{A_{\text{eff}}}\left(P_p\sqrt{\frac{P_s}{P_i}} + P_p\sqrt{\frac{P_i}{P_s}} - 4\sqrt{(P_sP_i)}\right)\sin\theta \quad \text{(1d)}$$

where P_m and $k_m, m = \{p, s, i\}$ represent the powers and propagation constants of the pump, signal, and idler waves, n_2 is the optical Kerr coefficient, $\beta_{2\text{PA}}$ is the two-photon absorption (2PA) coefficient, ω is the optical center frequency, and $\theta(z)$ represents the local phase mismatch between the three interacting waves. $\beta_{2\text{PA}}$ was measured separately to be 15 cm/GW, using the inverse transmission method, and the linear propagation loss (α) was measured to be 6 dB/cm. The wavevector mismatch is given by $k_s + k_i - 2k_p = -(2\pi c/\lambda^2)D\Delta\lambda^2$, where D is the group-velocity dispersion and $\Delta\lambda$ is the wavelength detuning between the signal and pump.

Fig. 2 shows the measured and calculated conversion efficiencies as functions of wavelength detuning $\Delta\lambda$. In this measurement, the pump and signal were generated from two tunable continuous-wave (CW) lasers. Both pump and signal were combined and coupled to the waveguide using a lensed fiber. The coupled input powers were estimated to be 22 and 19 dBm, respectively, and the total insertion loss was measured to be 8.7 dB, including 3 dB of coupling loss per facet. We define the FWM conversion efficiency to be the ratio between the idler and the signal power at the output of the waveguide. The 3-dB conversion bandwidth has a half-width of 24 nm. The inset of Fig. 2 shows the output spectrum from the waveguide for the pump–signal detuning of 5 nm, showing an FWM conversion efficiency of -28 dB. This figure falls to -31 dB if one accounts for the linear propagation loss (47%) and 2PA loss (6%) in the waveguide. The nonlinear efficiency in our devices is presently limited by propagation loss. Recently, submicrometer GaAs–AlGaAs waveguides have been fabricated with a propagation loss as low as 0.9 dB/cm at 1550 nm [12]. If one assumes the same optical Kerr coefficient for GaAs, the waveguides reported in [12] could potentially improve the conversion efficiency by +20 dB over what is reported here.

The solid line in Fig. 2 shows the results obtained by numerically integrating (1a)–(1d). n_2 can be obtained from the maximum conversion efficiency and was estimated to be 2.9×10^{-13} cm^2/W, comparable to the value of 1.59×10^{-13} cm^2/W reported in [5]. We attribute the discrepancy to a pump–signal polarization mismatch and to an uncertainty in the coupling efficiencies at the input and output facets. The limited bandwidth of the EDFAs precluded the measurement of the FWM conversion efficiency beyond 30 nm. The dispersion D was estimated to be -1340 ps/(nm $\cdot$ km) based on the observed conversion bandwidth together with a numerical calculation of modal and material dispersion of the waveguide. Increasing the device length or decreasing the mode area would improve the device performance, but may require optimization of the waveguide dispersion to maintain a wide bandwidth [13], [14].

The experimental setup for the NRZ-to-RZ conversion using FWM is shown in Fig. 3. The NRZ on–off keying (NRZ-OOK) data signal at the wavelength of 1545 nm was generated by modulating the output from a CW laser with a $2^{31} - 1$ pseudorandom bit sequence. The 10-GHz clock pulse train was generated from an actively mode-locked laser diode centered at 1553.5 nm with the pulsewidth of 3 ps. The NRZ signal and the clock pulse train were combined and coupled into the waveguide using a lensed fiber. The average coupled input powers for the NRZ-OOK signal and the clock pulse train were estimated to be 23 and 13.6 dBm, respectively. The signal emerging from the waveguide was collected using a second lensed fiber and bandpass-filtered by a 2-nm tunable grating filter to spectrally isolate the generated RZ-OOK idler. The preamplified receiver is composed of a low-noise EDFA, a 1-nm bandpass filter, a power EDFA, and a 2-nm bandpass filter. The detected signal was amplified in a transimpedance amplifier prior to BER evaluation.

Fig. 4 shows the optical spectrum at the output of the waveguide. The converted RZ-OOK signal was generated at 1536.5 nm for a pump–signal detuning of 8.5 nm, which was within the range where the FWM conversion efficiency was flat. The dashed trace in Fig. 4 represents the spectral profile of the composite filter, which includes the grating filter and the two filters in the receiver.

Fig. 5(a) and (b) show the eye diagrams of the baseline and converted RZ-OOK signals, respectively. The RZ-OOK

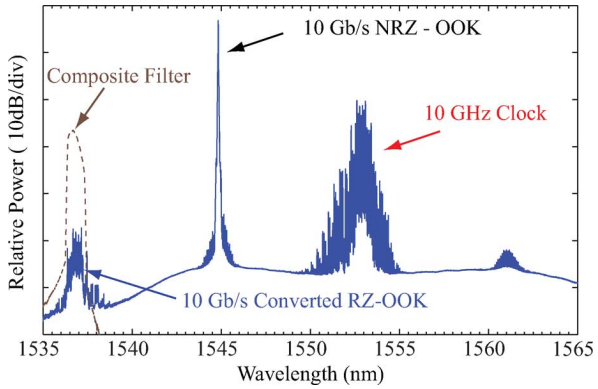

Fig. 4. Optical spectrum of the output signal from the waveguide (solid line) and the spectral profile of the bandpass filter (dashed line).

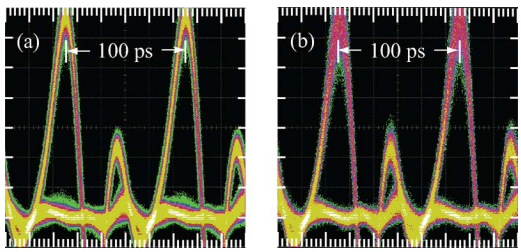

Fig. 5. Infinite-persistence sampling oscilloscope traces of (a) the baseline RZ-OOK signal, and (b) the converted RZ-OOK signal. Each trace was captured at −25-dBm receiver power, using a 10-Gb/s sampling module.

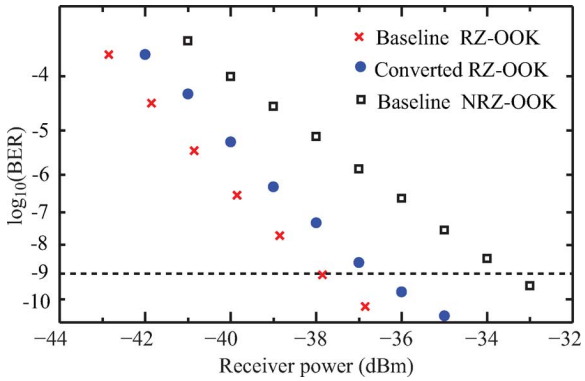

Fig. 6. BER versus receiver power for the 10-Gb/s wavelength converted signal, compared to the baseline RZ-OOK measurement, and the baseline NRZ-OOK measurement.

baseline was generated by modulating the 10-GHz clock. The converted signal quality shows only a modest degradation in comparison to the baseline performance. Fig. 6 depicts the receiver sensitivity measurement of the format conversion from NRZ-OOK to RZ-OOK. The converted RZ-OOK signal shows a receiver sensitivity penalty of 1 dB relative to the baseline RZ-OOK signal and a 3-dB improvement over baseline NRZ-OOK. The latter reflects the inherent performance gain of RZ compared to NRZ.

III. Conclusion

We have demonstrated, for the first time, 10-Gb/s wavelength and format conversion based on FWM in a GaAs bulk-waveguide. A conversion efficiency of −28 dB over a 48-nm bandwidth was achieved in a GaAs ridge waveguide with a relatively large effective area. The converted RZ-OOK signal exhibited a penalty of 1 dB relative to a baseline RZ-OOK signal and a gain of 3 dB relative to baseline NRZ-OOK at 10^{-9} BER. The FWM conversion efficiency could be further improved by reducing the propagation losses and optimizing the bandgap to suppress 2PA. Nonetheless, this report demonstrates the viability of GaAs–AlGaAs waveguides for nonlinear optical signal processing.

References

[1] J. H. Lee, W. Belardi, K. Furusawa, P. Petropoulos, Z. Yusoff, T. M. Monro, and D. J. Richardson, "Four-wave mixing based 10-Gb/s tunable wavelength conversion using a holey fiber with a high SBS threshold," *IEEE Photon. Technol. Lett.*, vol. 15, no. 3, pp. 440–442, Mar. 2003.

[2] X. Yang, A. K. Mishra, R. J. Manning, R. P. Webb, and A. D. Ellis, "All-optical 42.6 Gbit/s NRZ to RZ format conversion by cross-phase modulation in single SOA," *Electron. Lett.*, vol. 43, no. 16, pp. 890–892, 2007.

[3] M. A. Foster, A. C. Turner, R. Salem, M. Lipson, and A. L. Gaeta, "Broad-band continuous-wave parametric wavelength conversion in silicon nanowaveguides," *Opt. Express*, vol. 15, no. 20, pp. 12949–12958, 2007.

[4] W. Astar, J. B. Driscoll, X. Liu, J. I. Dadap, W. M. J. Green, Y. A. Vlasov, G. M. Carter, and J. R. M. Osgood, "Conversion of 10 Gb/s NRZ-OOK to RZ-OOK utilizing XPM in a Si nanowire," *Opt. Express*, vol. 17, no. 15, pp. 12987–12999, 2009.

[5] M. Dinu, F. Quochi, and H. Garcia, "Third-order nonlinearities in silicon at telecom wavelengths," *Appl. Phys. Lett.*, vol. 82, no. 18, pp. 2955–2957, 2003.

[6] A. Villeneuve, C. C. Yang, G. I. Stegeman, C. N. Ironside, G. Scelsi, and R. M. Osgood, "Nonlinear absorption in a GaAs waveguide just above half the band gap," *J. Quantum Electron.*, vol. 30, no. 5, pp. 1172–1175, 1994.

[7] A. Villeneuve, K. AI-Hemyari, J. U. Kang, C. N. Ironside, J. S. Aitchison, and G. I. Stegeman, "Demonstration of all-optical demultiplexing at 1555 nm with an AlGaAs directional coupler," *Electron. Lett.*, vol. 19, no. 8, pp. 721–722, 1993.

[8] P. P. Absil, J. V. Hryniewicz, B. E. Little, P. S. Cho, R. A. Wilson, L. G. Joneckis, and P.-T. Ho, "Wavelength conversion in GaAs micro-ring resonators," *Opt. Lett.*, vol. 25, no. 8, pp. 554–556, 2000.

[9] K. Inoue, H. Oda, N. Ikeda, and K. Asakawa, "Enhanced third-order nonlinear effects in slow-light photonic-crystal slab waveguides of line-defect," *Opt. Express*, vol. 17, no. 9, pp. 7206–7216, 2009.

[10] G. A. Siviloglou, S. Suntsov, R. El-Ganainy, R. Iwanow, G. I. Stegeman, and D. N. Christodoulides, "Enhanced third-order nonlinear effects in optical AlGaAs nanowires," *Opt. Express*, vol. 14, no. 20, pp. 9377–9384, 2006.

[11] K. Inoue and T. Mukai, "Signal wavelength dependence of gain saturation in a fiber optical parametric amplifier," *Opt. Lett.*, vol. 26, no. 1, pp. 10–12, 2001.

[12] J. Shin, Y.-C. Chang, and N. Dagli, "Propagation loss study of very compact GaAs/AlGaAs substrate removed waveguides," *Opt. Express*, vol. 17, no. 5, pp. 3390–3395, 2009.

[13] J. Meier, W. S. Mohammed, A. Jugessur, L. Qian, M. Mojahedi, and J. S. Aitchison, "Group velocity inversion in AlGaAs nanowires," *Opt. Express*, vol. 15, no. 20, pp. 12755–12762, 2007.

[14] F. Luan, M. D. Pelusi, M. R. E. Lamont, D.-Y. Choi, S. Madden, B. Luther-Davies, and B. J. Eggleton, "Dispersion engineered As_2S_3 planar waveguides for broadband four-wave mixing based wavelength conversion of 40 Gb/s signals," *Opt. Express*, vol. 17, pp. 3514–3520, 2009.